Seismic Source Characterizations of Northern California Earthquakes through Moment Rate Function Properties

T. Taira, D.S. Dreger (Berkeley Seismological Laboratory)

Summary

- We compile moment rate functions (MRFs) of small to moderate earthquakes (3 <= M <= 6) for northern California through an empirical Green's function approach with the aim to systematically evaluate radiate energy and also rupture complexities.
- Our analysis finds total 235 EQs (3.0 < M < 5.1; 2.6km < depth < 18km) that have a suitable eGf event to evaluate their MRFs.
- We are particulariy interested in exploring if the moment-scaled radiated energy depends on seismic moment, i.e., if our data set can be explained by whether self-similarity or non-self-similarity scaling.
- Our results suggest a weak non-self-similarity behavior, which appears to be consistent with results from Kanamori and Rivera (2004, BSSA) that analyzed southern California earthquakes.
- No clear spatial and depth variations is found for scaled energy from our MRF dataset.
- We also performed a finite-fault modeling for subsets of earthquakes by inverting MRFs including the 2022 Mw 5.06 Alum Rock earthquake. This earthquake exhibits a complex rupture process involving three subevents with a southeast directivity.
- The peak and median slips are found to be 42 cm and 14 cm respectively, which provides the peak and median static stress drop of 28 MPa and 5 MPa.
- Estimated moment magnitudes for three subevents are 4.46, 4.78, 4.67, which are equivalent to 12%, 38%, and 26% of the total seismic moment.
- Seismic radiation efficiency is estimated to be 1.76, which is comparable with those of other crustal earthquakes such as the 1992 Mw 7.3 Landers and the 1994 Mw 6.7 Northridge earthquakes.

Source Parameters and Scaling Relations

Scaled Energy with Seismic Moment

- self-similarity -> E_R/M_0 is scale independent

$$e_R = \frac{E_R}{M_o} \sim M_o^{\varepsilon/(3+\varepsilon)} \qquad \varepsilon = 0 \text{ -> self-similar model}$$

- Our results shows the scaled energy appear to be increases as a function of seismic moment, which suggests a weak non-self-similarity behavior.

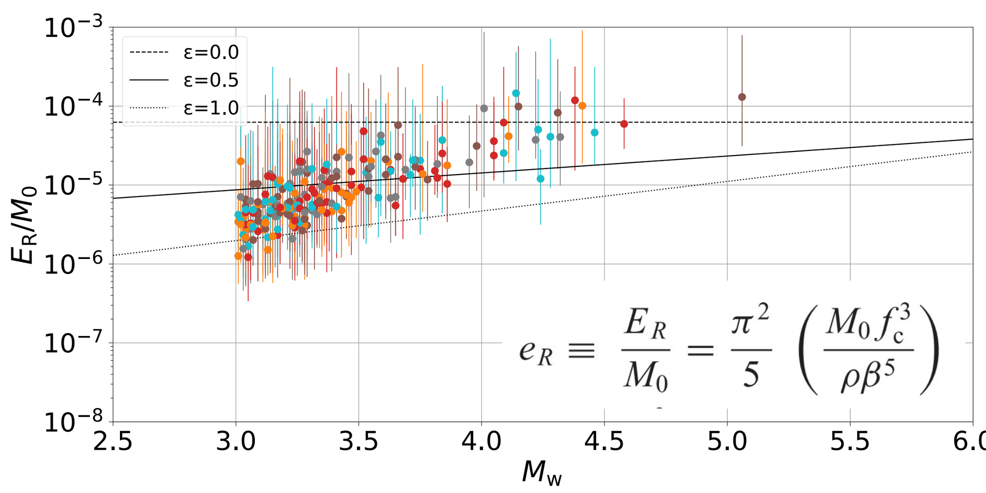

Figure 4: Scaled energy measurements from our 235 NCal earthquakes as a function of seismic moment (Mw).

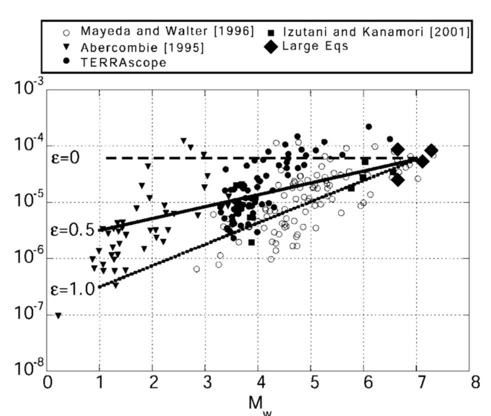

- Kanamori and Rivera (2004, BSSA) shows a similar weak non-self-similarity for southern California earthquake data.

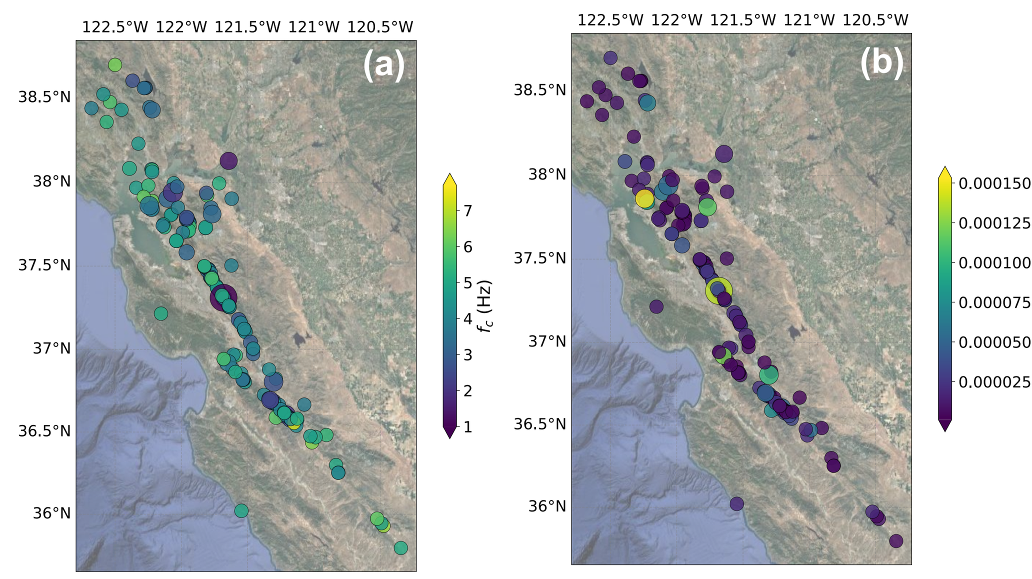

Figure 5: Map views of earthquakes with resultant (a) corner frequency and (b) scaled energy. No clear spatial variations of both parameters is found.

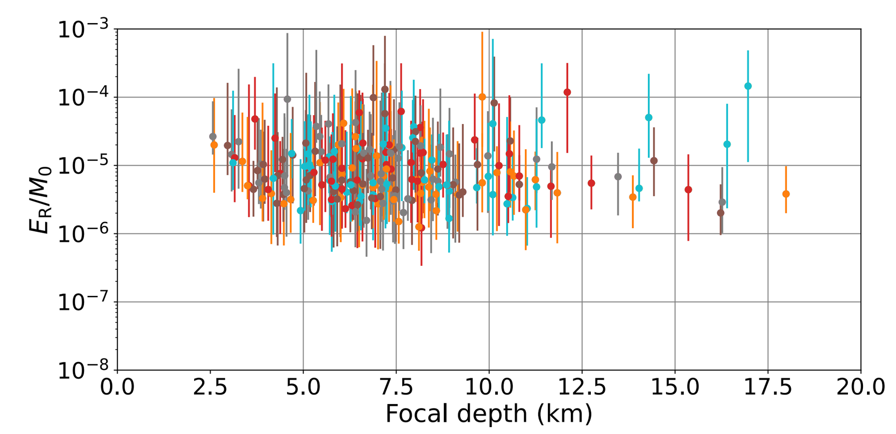

Figure 6: Scaled energy measurements from our 235 NCal earthquakes as a function of focal depth. No clear depth-dependency is found.

Developing Northern California Moment Rate Function Database

Empirical Green's Function (eGf) Analysis

- eGf event: co-located with a similar source mechanism with 1-2.5 M units smaller than the target EQ -> correcting path and site effects.

$$\frac{U_{\text{main}}(\omega)}{U_{\text{eGf}}(\omega)} = \frac{S_{\text{main}}(\omega)G_{\text{main}}(\omega)I(\omega)}{S_{\text{eGf}}(\omega)G_{\text{eGf}}(\omega)I(\omega)} = \hat{S}_{\text{main}}(\omega)$$

$$S(t) = \dot{M}(t) \text{ where } M_0 = \int_0^{\infty} \dot{M}(t)\,dt$$

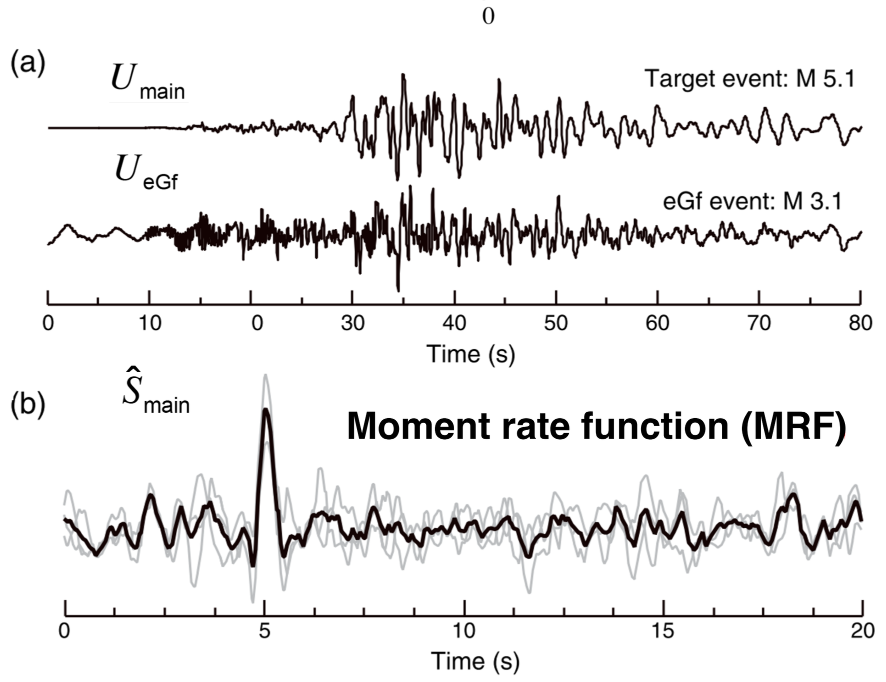

Figure 1: (a) Two seismograms (raw waveforms) from the 1998 Mw 5.1 San Juan Bautista earthquake (target event) and the nearby M 3.1 foreshock (eGf event) recorded at broadband station BK.BKS in the north-south component. The waveforms are normalized by their maximum amplitudes. (b) Moment rate functions (MRFs) obtained at station BK.BKS from three individual components (gray lines) through a deconvolution process. Also shown is the stacked MRF (black line) from those three MRFs.

Systematic Search for Target-eGf Pairs

1. Search for possible eGf events within 3 km hypocentral distance and 1-2.5 M units smaller than the target EQ.
2. Perform a deconvolution and then check resultant moment rate function data (signal-to-noise, SNR).
3. If at least 10 stations with SNR > 10, keep this target-eGf pair and load this pair in the database

- Total 235 EQs (3.0 < M < 5.1; 2.6km < depth < 18km) is found and we explore time domain characteristics of resultant MRFs.

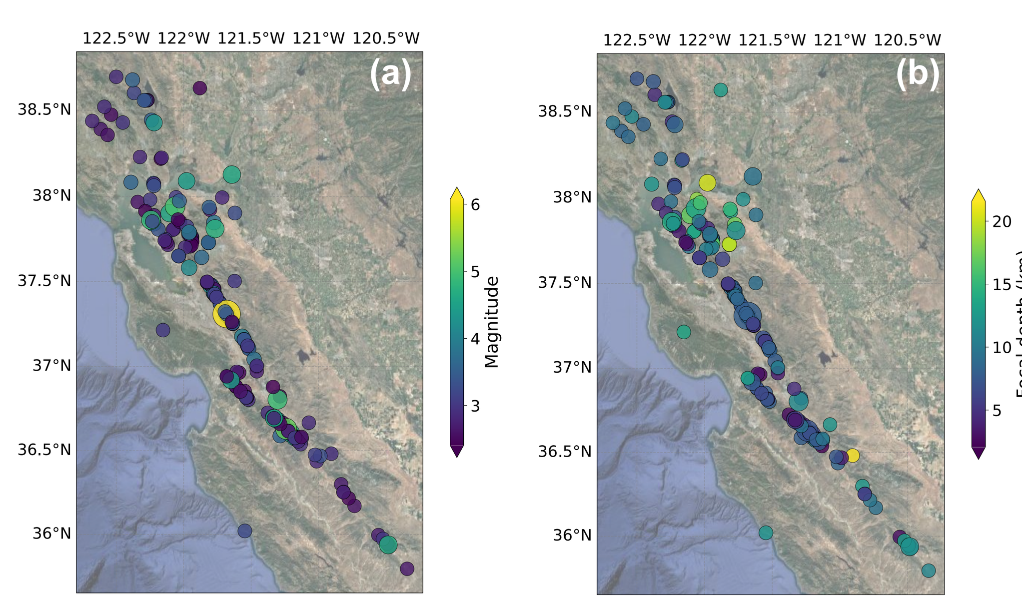

Figure 2: Map views of 235 northern California earthquakes where we find suitable eGf events sorted by (a) magnitude and (b) focal depth. The largest earthquake in our dataset is the 2022 Mw 5.06 Alum Rock earthquake.

Time-Domain Characteristics

- Our analysis focuses on the total energy and the durations of individual MRFs, which can be measured to radiated energy and corner frequency (and stress drop), assuming Brune's omega-squared model.

Radiated energy

$$E_R = \left(\frac{1}{15\pi\rho\alpha^5} + \frac{1}{10\pi\rho\beta^5}\right)\int \dot{M}^2(t)\,dt$$

Stress drop Assumption: circular crack model

$$\Delta\sigma = \left(\frac{875}{16c^3}\right)\mu\left(\frac{M_0}{\mu\beta^3 T^3}\right)$$

Duration and corner frequency relation

$$T = \frac{5}{2\pi f_c} \qquad \text{Assumption: omega-squared model}$$

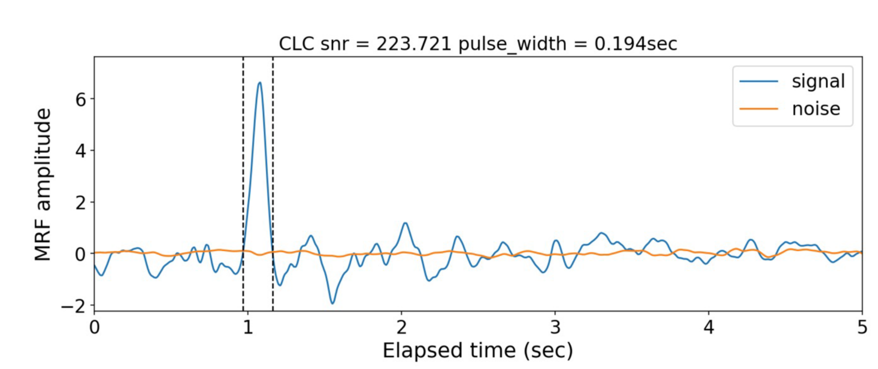

Figure 3: Example of MRF in noise and signal windows. Dashed lines show the duration window of the MRF.

Finite-Fault Modeling of the 2022 Alum Rock Earthquake

- A finite-fault modeling of the 2022 Mw 5.06 Alum Rock earthquake is performed by inverting MRFs (Dreger 1994).
- Single 10 km × 10 km plane and divide it into 3721 164 × 164 m subfaults.
- Variance reduction (VR) is used to evaluate the waveform fit.

$$VR = \left[1 - \frac{\int\{D(t) - S(t)\}^2 dt}{\int\{D(t)\}^2 dt}\right] \times 100$$

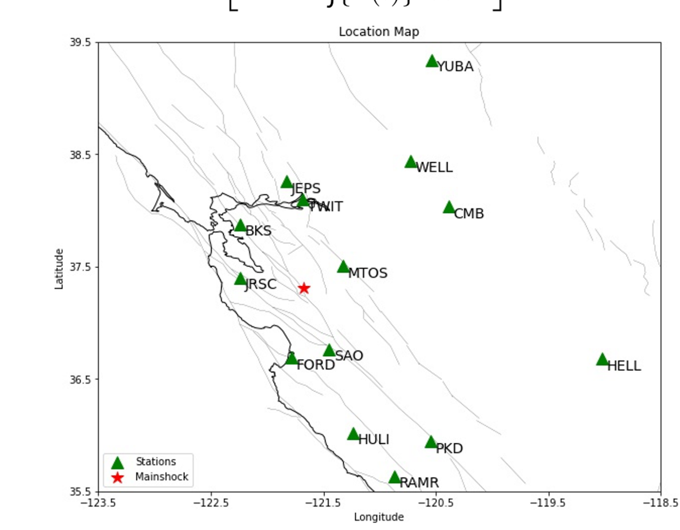

Figure 7: Map view of seismic station (total 14 sites) s used to perform a finite-fault modeling of the 2022 Mw 5.06 Alum Rock earthquake.

Rupture Directivity

- MRFs obtained at a set of broadband stations with a good azimuth coverage reveal a strong southward rupture directivity.

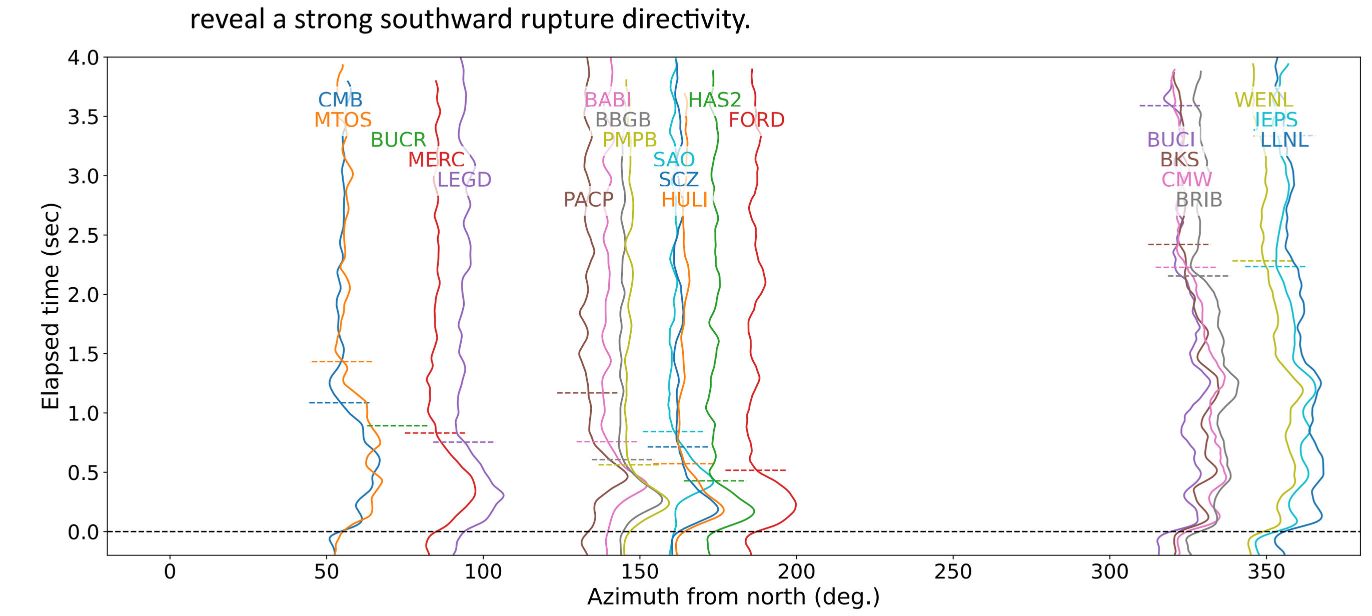

Figure 8: MRFs for the 2022 Mw 5.06 Alum Rock earthquake as a function of azimuth from the hypocenter. MRFs are aligned by the onset of the first pulse. Dashed lines show the end time of MRFs.

Sensitivity Analysis

- A best combination of parameters: rupture velocity = 3.3 kms, rise time = 0.07s, smoothing = 100, which provides VR = 72.96%.

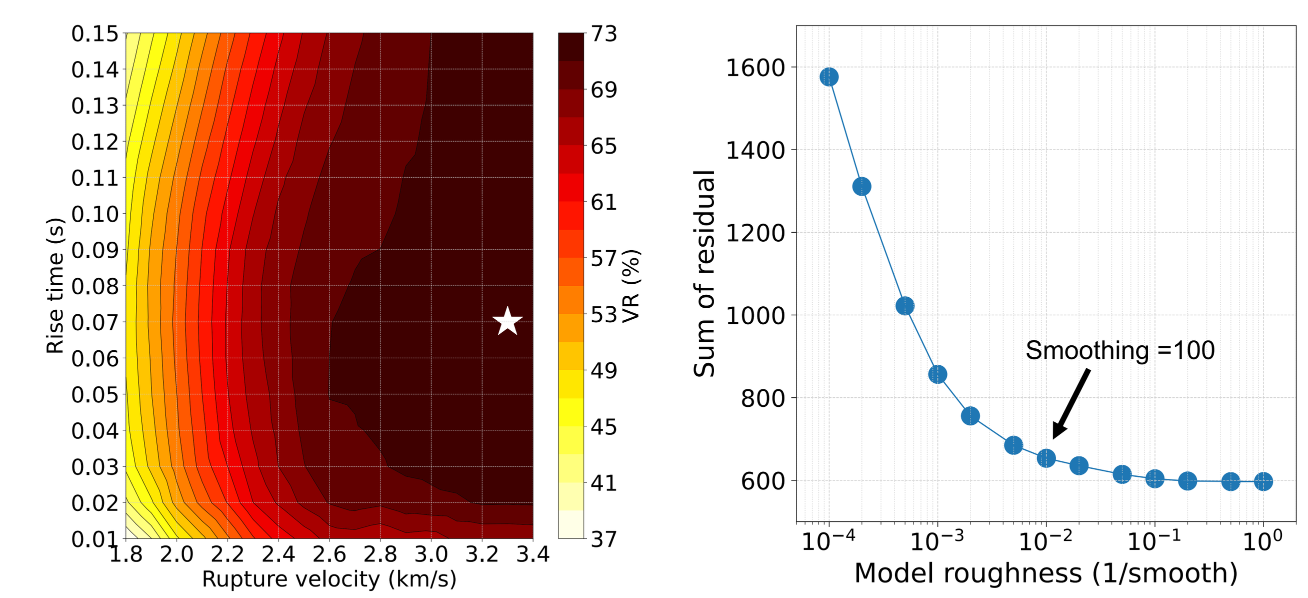

Figure 9: Sensitivity analysis of rupture velocity, rise time, and smoothing factor for the 2022 Mw 5.06 Alum Rock earthquake.

Coseismic Slip Model

- Three asperities (P1, P2, P3) found. >20 cm slip released.

Static Stress Drop

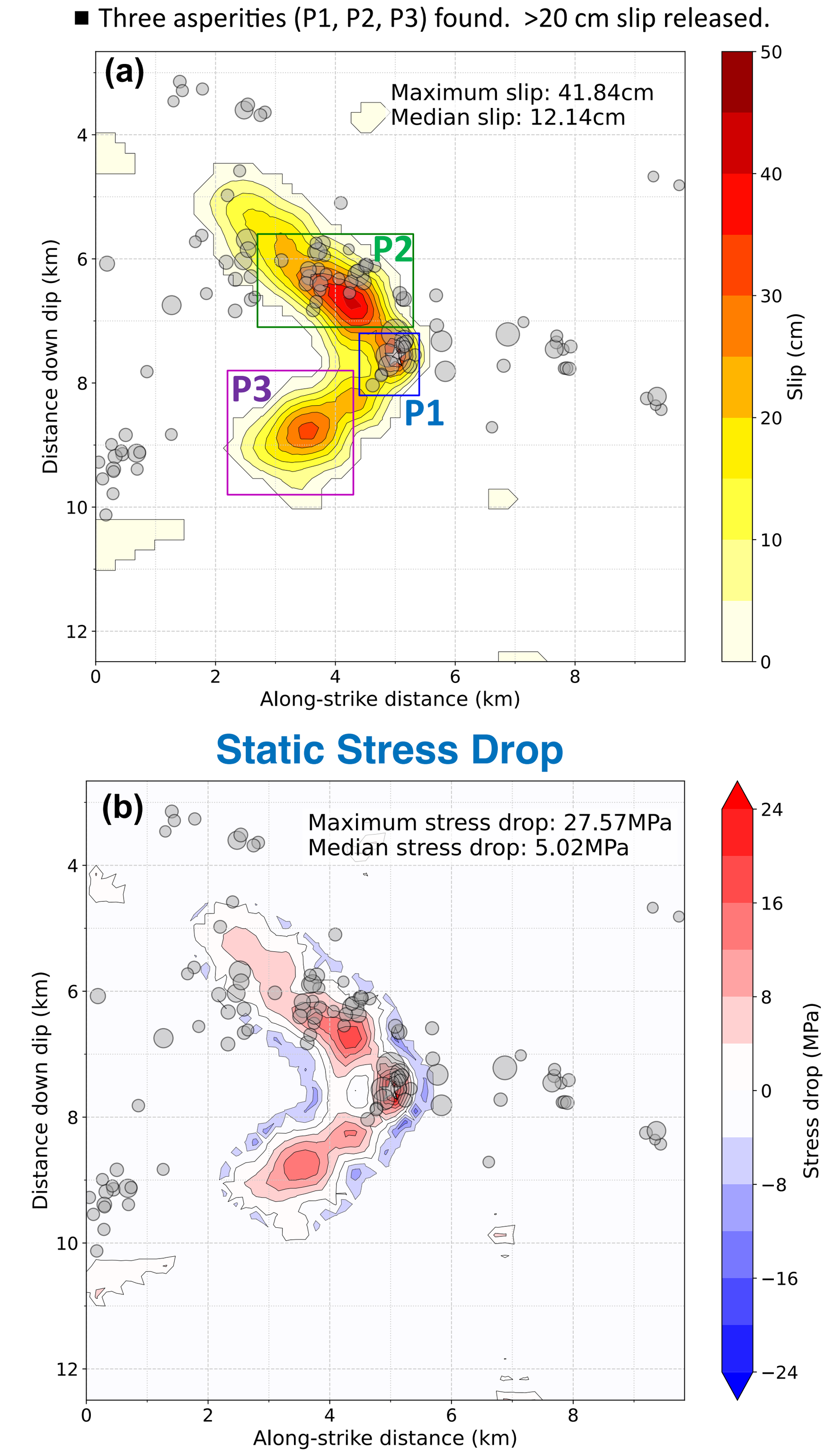

Figure 10: Spatial distributions of (a) fault slip and (b) static stress drop for the 2022 Mw 5.06 Alum Rock mainshock.

Forward Modeling

- To understand the contributions from individual asperities, forward modeling is performed.

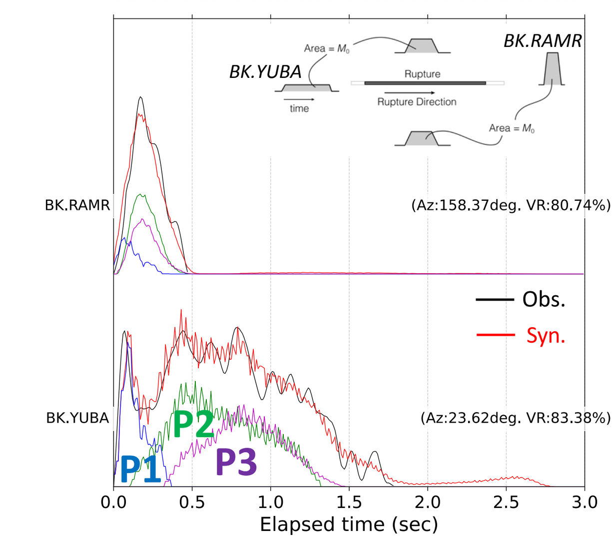

Figure 11: Examples of observed MRFs (black) from BK.YUBA and BK.RAMR with synthetic MRFs from the best-fit coseismic model.

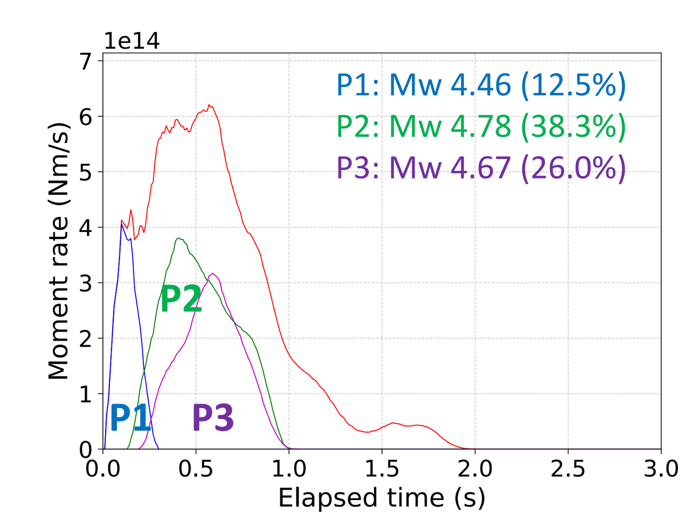

Figure 12: Composite moment rate function from the coseismic slip model. Also shown are these from three asperities.

Seismic Radiation Efficiency

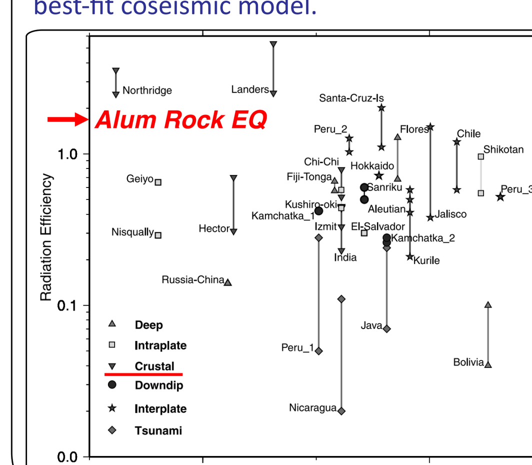

$$\eta_R = E_R/E_{T0} = (5.00e{+}12/2.84e{+}12) = 1.76$$

Radiated energy :from the composite MRF (Fig. 12).

$$E_R = \left(\frac{1}{15\pi\rho\alpha^5} + \frac{1}{10\pi\rho\beta^5}\right)\int \dot{M}^2(t)\,dt$$

Elastic energy :from the spatial distribution of coseismic slip (Fig. 10).

$$E_{T0} = \frac{1}{2}\int \Delta\sigma_s D A$$

Acknowledgments

- Waveform data, metadata, and earthquake catalog for this study were accessed through the Northern California Earthquake Data Center (NCEDC).